UCRL-ID-132866

Measurements at 351 nm of temporal dispersion in fibers

David Milan
Calvin Thompson
Walter Sell
Roger Griffith

November 4, 1998

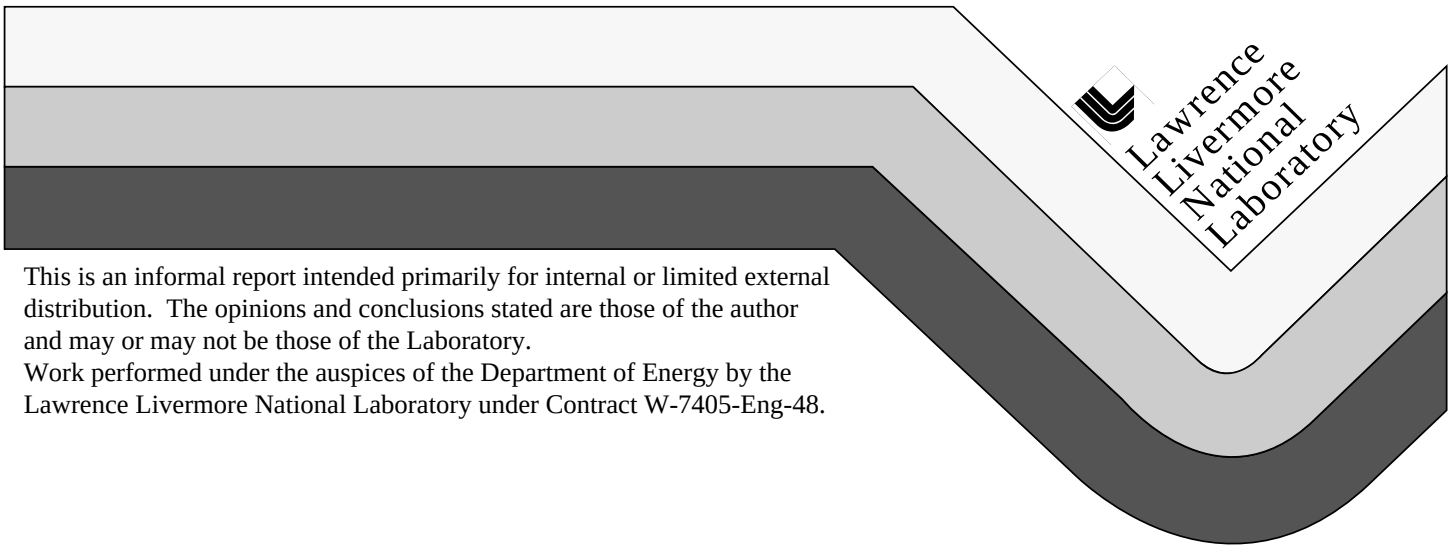

Work performed under the auspices of the Department of Energy by the Lawrence Livermore National Laboratory under Contract W-7405-Eng-48.

National Ignition Facility Project

Mail Stop L-483

Ext: 2-5499

November 4, 1998
NIF # 0016173
WBS 1.7.2.2

TO: Distribution

FROM: David Milam, Calvin Thompson, Walter Sell, Roger Griffith

SUBJECT: Measurements at 351 nm of temporal dispersion in fibers.

I. Summary.

1. Temporal dispersion at 351-nm was measured in the following: a 35-m bundle of 19 each 50-μm-core fibers, a companion 35-m single fiber, a 100-μm-core single fiber (at 4 lengths), and a 50-μm-core single fiber (two samples, 7 lengths). The 50-μm-core fiber was from preform #24; the 100-μm-core fiber was a prototype version having a thick cladding. All of the fibers were developed and manufactured at the Vavilov State Optical Institute, St. Petersburg, Russia.

2. Dispersion measurements were made by propagating a 20-ps 351-nm pulse through the fiber under test and recording the output on an S20 streak camera. The width of the pulse transmitted by the fiber was compared to that of a fraction of the pulse that had propagated over an air path. Values of dispersion were calculated as, $D = \sqrt{\left(F^2 - A^2\right)}$, where F and A are the full widths at half maximum (FWHM) for, respectively, the fiber-path and the air-path streaks.

3. In each of the experiments, the measured dispersion increased with counts in the streak record, which in principle, are proportional to intensity in the fiber. Measured values of dispersion ranged from about 0.6 to 1.0 ps/m for the single fibers.

4. The measured FWHMs of both the fiber-path pulse and the air-path pulse increased with increase in counts in the streak record. The rate of broadening was greatest for the fiber-path pulse, and the broadening of that pulse was the primary cause for the dependence of dispersion on counts in the streak record. Pulse broadening with increase in counts is symptomatic of camera saturation, but it is difficult to understand why saturation should have effected the fiber-path pulses more strongly.

5. There were spatial anomalies in the streak records of the output pulses from some of the fibers. Emission by the bundle of a "doubled" pulse is a primary example. In streaks recorded at about 800 counts, the total duration for the pair of pulses was about 100 ps. The maxima of the pulses occurred in different columns of the streak, so there was a relative spatial or angular offset between the two pulses.

Pulses with extended tails were observed in each streak that was recorded at about 400 counts.

6. We frequently had difficulty obtaining adequate transmittance through 50-μm single fibers. Some of our problems probably were related to inexperience in cleaving this particular fiber.

II. Test arrangement.

A schematic of the arrangement is shown in Fig. 1. A single 125-ps, 1053-nm pulse was selected from a mode-locked train that was emitted by a Nd:YLF oscillator, and injected into a chirping fiber. The 16-nJ output from this fiber was injected into the front end of the OSL chain which amplified the pulse energy to 4 mJ and relayed the pulse to the compressor gratings. Compression provided 1053-nm, 20-ps, 1-mJ pulses, which were converted by tripling in KDP crystals into 40-μJ, 351-nm pulses.

One half of the energy in the 351-nm pulse was injected into a UV Launch Optic [Ref. 1]which was attached by an SMA coupler to the fiber under test. The remainder of the UV light propagated over an air path. Each streak record contained light from both of these channels. Color filters were used to prevent entry of 527-nm or 1053-nm light into the fibers.

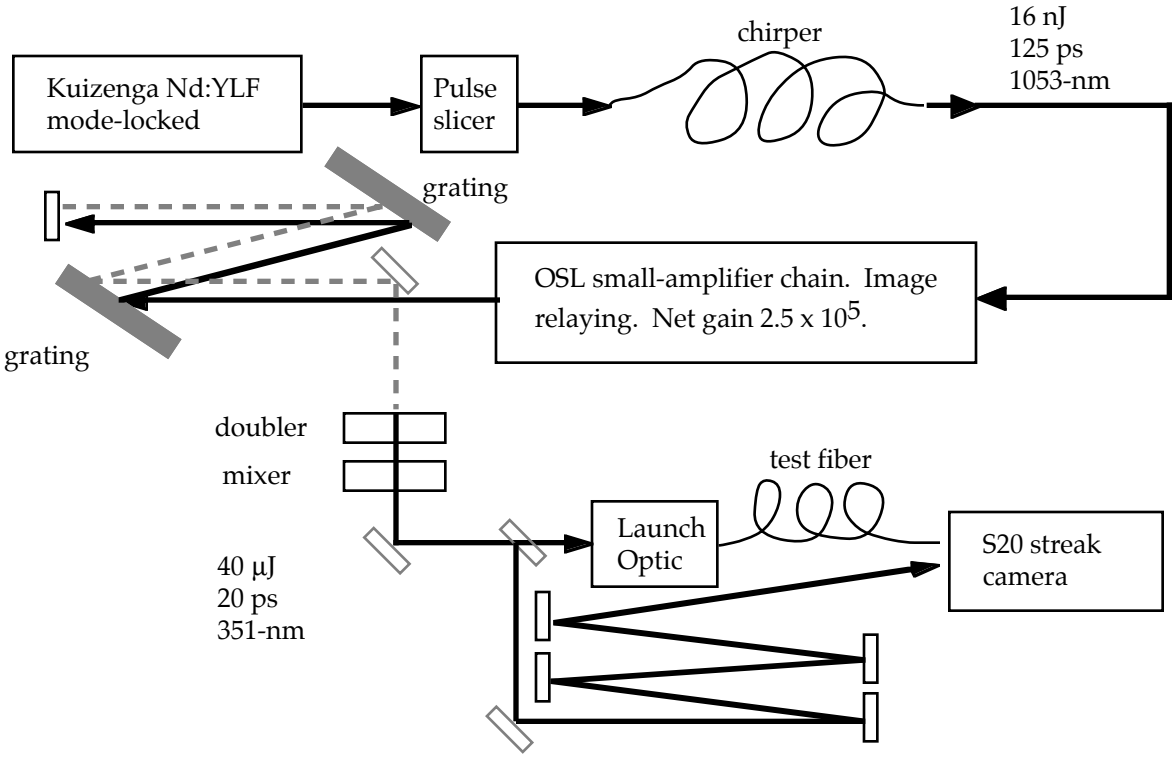

Fig. 1. Diagram of the arrangement for measuring dispersion at 351 nm in optical fibers.

During the course of the experiment, the only significant variation was in the manner of coupling light into the streak camera. Two fixtures for holding the end of a fiber in the entrance slit of the camera were available. One had two SMA bulkhead couplers. The test fiber was connected to one coupler, and light from the air path was injected through the hole in the other coupler. Figure 2 shows a representative streak. Light from the air path, with diffraction caused by passage of the light through the SMA connector, is in the left half of the streak. Light from the fiber is in the right half.

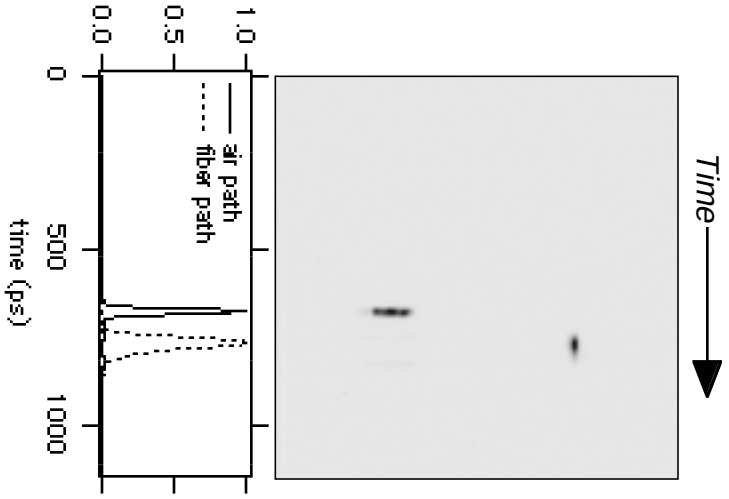

Fig. 2. Streak typical of those recorded when the output end of the test fiber was equiped with an SMA connector.

The second fixture was a slotted bar for clamping unconnectorized fibers. It occupied about one half of the camera slit. Figure 3 shows a representative streak. In this instance, light from the air path was injected through the unoccupied half of the camera slit, and a wedged attenuator was placed over one half of the beam.

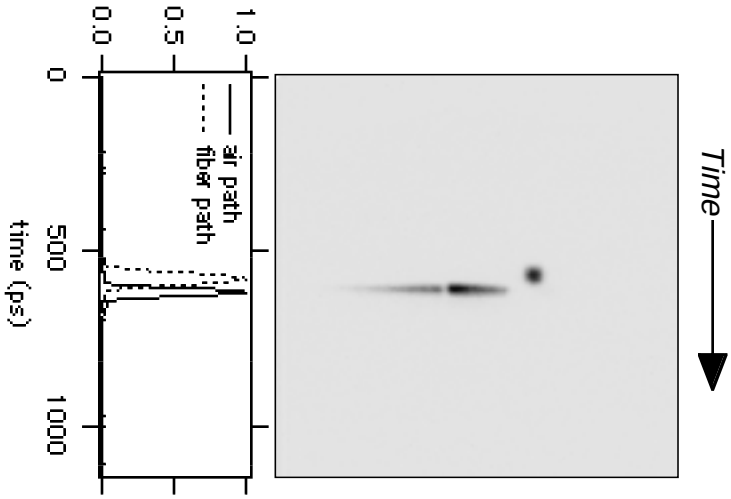

Fig. 3. Streak typical of those recorded when the output end of the fiber was not connectorized.

The time sweep of the streak camera was calibrated against rattle-down pulses from a 2.54-cm silica etalon with reflective faces. The resulting curve is shown in Fig. 4. The sweep rate is about 2 ps/pixel, and the useable portion of the sweep is about 1000 ps in duration.

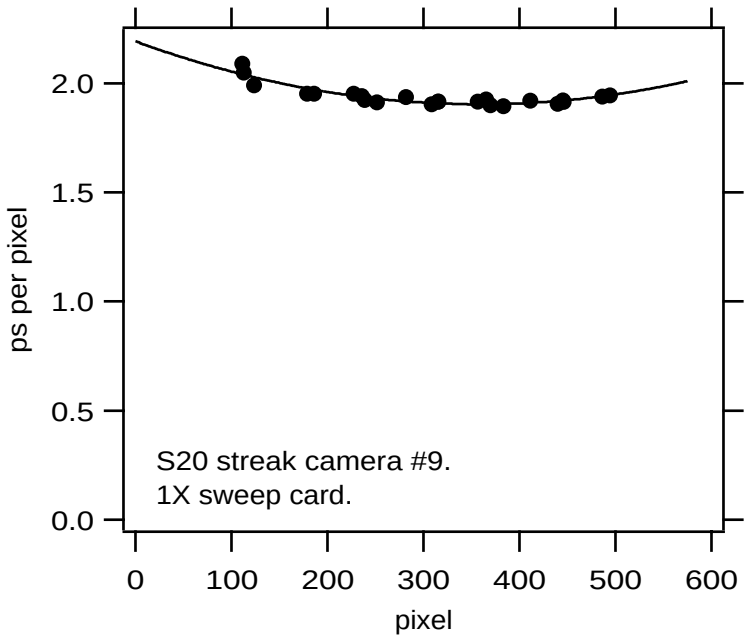

Fig. 4. Calibration of the streak camera.

III. Reduction of the data.

In principle, reduction of the data was simple. We decided to characterize the dispersion by a simple equation, $D = \sqrt{\left(F^2 - A^2\right)}$, where F and A are the full widths at half maximum (FWHM) for, respectively, the fiber-path streak and the air-path streaks. Therefore, measurement of FWHM was all that was required. However, the uncertainties indicated by a first pass through the data were much larger than expected. The origin of the large uncertainties was identified by analyzing the variation of FWHM with counts in the streak record.

These general observations characterize all of the data from this experiment.
(1) The air-path streak exhibited a variation of FWHM with both spatial location in the beam and with counts in the streak. These variations increased the measurement uncertainty and caused the FWHM to increase slightly with counts.
(2) The fiber-path streaks were more varied. Some were spatially uniform in appearance, and for these the FWHM was spatially uniform. Others exhibited strong spatial variation of FWHM. In general, the measured FWHM increased rapidly with increase in camera counts.
(3) The calculated dispersion varied with counts in the fiber-path streak, but was almost independent of counts in the air-path streak.
(4) The range in values of dispersion for a particular experiment was usually greater than the uncertainty in individual measurements.

III.A. Assignment of FWHM to air-path streaks.

Consider first the assignment of FWHM to air-path streaks like the one shown in Fig. 3. Because the camera observed the entire beam, and half of the beam was covered by a filter, waveforms can be generated from column lineouts with varied counts. Pulse duration measured in the high-count beam center usually were greater than durations that were determined in the low-intensity skirt of the beam. In the first few streaks that were examined, the center-to-skirt ratio varied from 1 to 1.5, so it seemed possible to select shots for which the FWHM was unambiguous.

To this end, eight waveforms were generated for each air-path streak. Each was an average of 3-5 columns. Two examples of the results are shown in Figs. 5 and 6. The line graph in each of these figures is a single row from the streak, so the graph is intensity (counts) vs column number and not a temporal waveform. The left half of the streak was attenuated by a tapered-thickness AR-coated wedge of NG-11. The attached tags give the values of FWHM that were measured from columns centered at the location of the tag.

For the data shown in Fig. 5, the measured pulse duration was about 20 ps in the skirts of the beam, and about 26 ps at the center of the beam. The fact that the pulse duration in the center of the beam is independent of counts indicates that the spread of measured widths is a property of the beam, and not camera saturation.

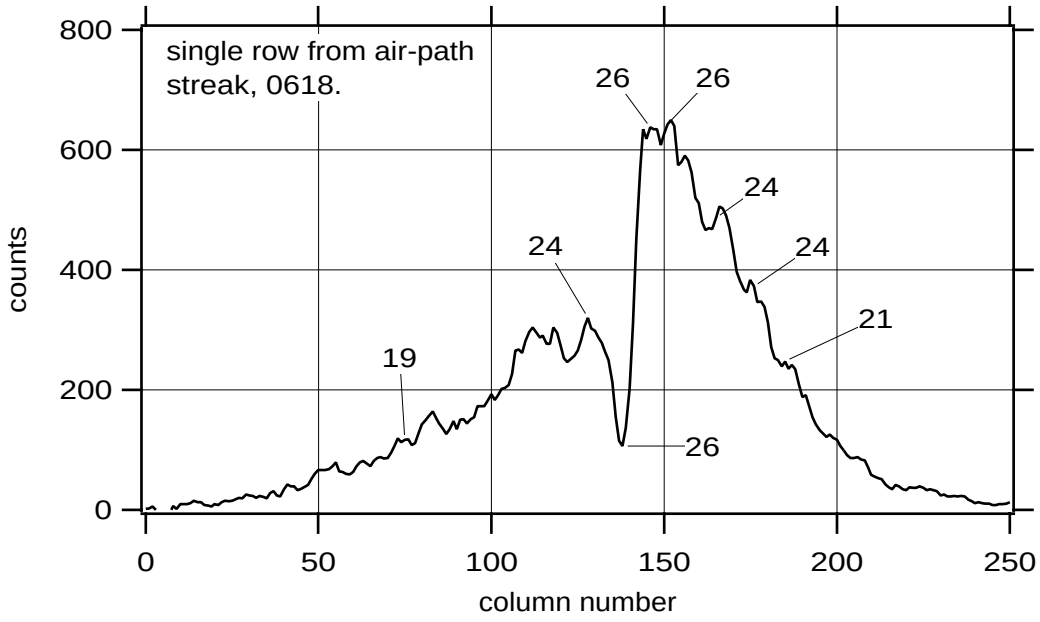

Fig. 5. Row from an air-path streak. Each tag gives the value in ps of the FWHM that was measured from a 3-column average centered at the tagged position.

A pulse broadening that could be attributed to camera saturation is shown in

Fig. 6, which contains a row cut from a more intensely exposed streak. In the center of the beam, the durations were 35 ps at 2000 counts and 28 ps at 400 counts. In both skirts, the duration was 23 ps. The total spread in pulse duration could be interpreted as 5 ps of difference between the edge and center of the beam, with 7 ps of saturation broadening at the beam center.

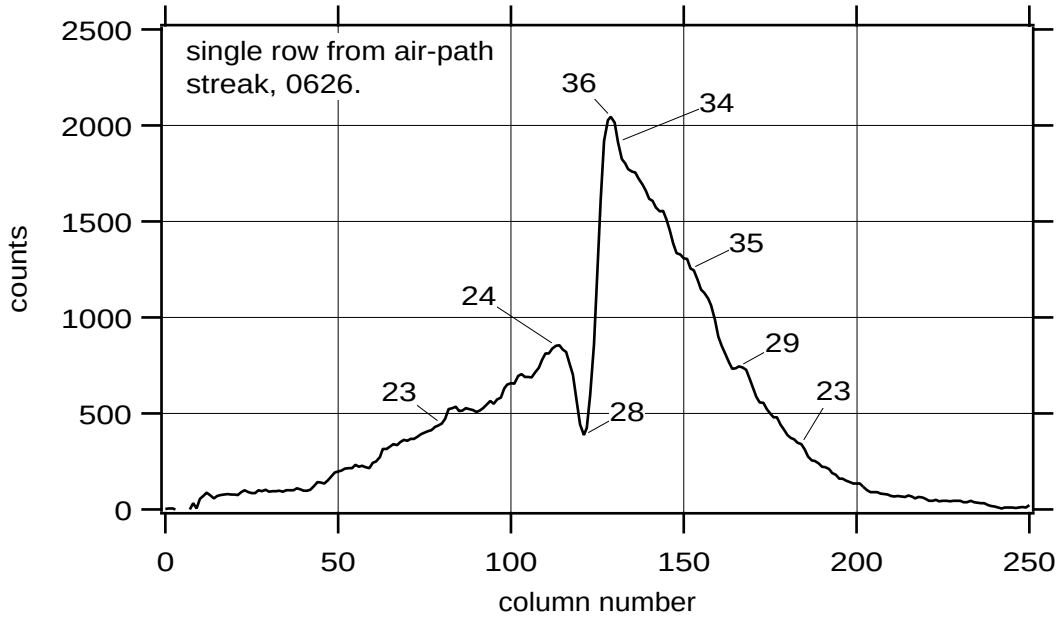

Fig. 6. Row cut from a more heavily exposed streak. The strong dependence of measured width on counts is symptomatic of camera saturation.

We decided to define the FWHM for air-path streaks as the average of four values measured from lineouts at varied counts. The selected lineouts were from the unattenuated half of the streak. Figure 7 contains the values of FWHM from the experiment that contained the greatest range in counts in the air-path streak. It is a rather surprising result. The values of FWHM that were assigned by this averaging did not vary strongly with camera counts, but the uncertainty did.

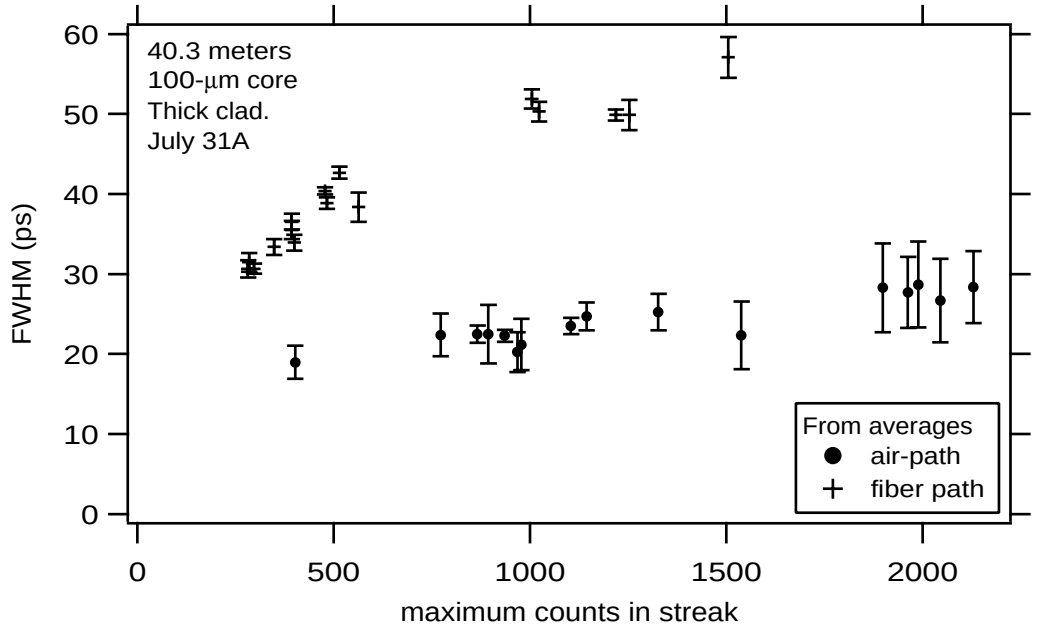

Fig. 7. Measured values of FWHM as a function of the maximum counts in the streak record.

III.B. Assignment of FWHM to Fiber-path streaks.

The fiber-path streaks contain only a few columns of data, so studies of FWHM vs counts were done with lineouts that contained only one column. Fiber-path streaks and row lineouts across these streaks are shown in Figs. 8 and 9. These streaks are extremes. In Fig. 8 is a streak recorded at 2200 counts. It is spatially symmetric, and waveforms from anywhere within the streak had approximately the same FWHM.

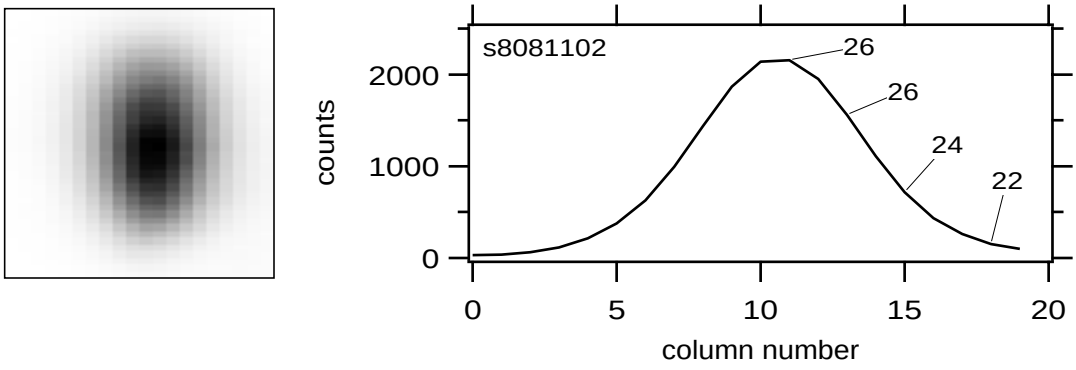

Fig. 8. Spatially symmetric fiber-path streak. Left: Excerpted segment of the streak. Duration (top to bottom) is 160 ps. Right: Row cut with tags which give the values of FWHM that were measured at the tagged locations.

The streak in Fig. 9 was recorded at only 800 counts, but it is not spatially uniform. The FWHM is much greater at the center than in the left skirt.

We defined the width of the fiber-path streaks to be the average four values of FWHM that had been measured from columns with differing counts. Figure 7 contains the FWHMs that were measured for the July 31 data set. Here the situation is exactly the reverse of that for air-path streaks. For spatially symmetric fiber-path streaks, the assigned values of FWHM varied significantly with counts, but uncertainties in individual values did not. At present, there is not an explanation for the behavior of the fiber-path streaks.

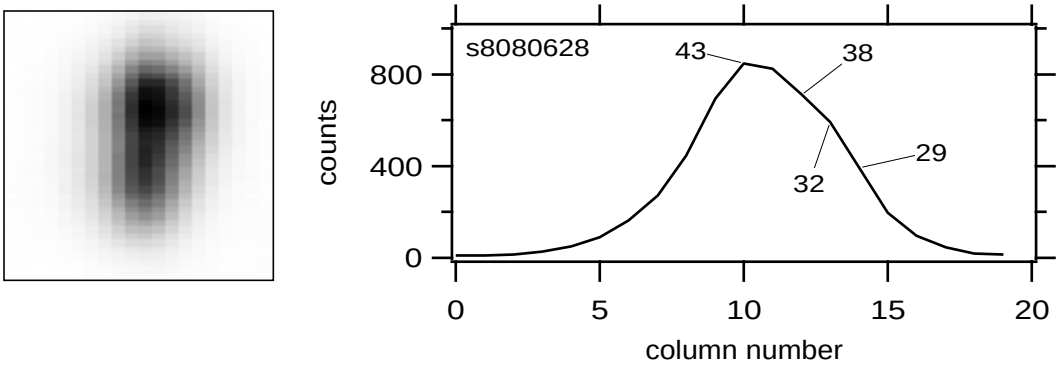

Fig. 9. Example of a streak that was not spatially symmetric.

III.C. Uncertainties.

For an individual FWHM, the assigned uncertainty is the full range of the four values of FWHM that were averaged. In some cases, this range was less than the 1-ps precision of the experiment.

For an individual value of dispersion, the assigned uncertainty is the full range that is allowed by the assigned uncertainties in the particular pair of FWHMs. The dominant contribution to the uncertainty in dispersion was the dependence of the FWHM of the fiber-path streak on camera counts.

IV. Tests of a 35-meter bundle and a companion 35-meter single fiber.

We tested a 35-m bundle that contained 19 each 50-μm-core fibers, and companion 35-m length of the fiber. SMA connectors were mounted on both ends of the bundle and the fiber. The lengths of the fibers in the bundle were measured by mechanical rather than optical means. This was done as part of the bundle development effort to reduce projected bundle fabrication costs.

IV. A. Results for the 35-m single fiber.

The fiber-path streaks were spatially symmetric, and they were recorded with only slight variation in counts, 550 to 830. The air-path streaks were recorded at 490 to 1640 counts. Expanded images of one air-path and one fiber-path streak are shown in Fig. 10. The measured values of FWHM are shown in Fig. 11. With a

single exception, the range in the four values of FWHM for each pulse was less than 1 ps.

Figure 12 contains the calculated dispersions. For this fiber, the data are nicely clustered, so it makes sense to define the dispersion to be the mean, 33 ps, with standard deviation of 1.7 ps. This corresponds to about 33 ps/35 m = 0.94 ps/m.

However, data presented below for other 50-μm fibers suggest that the uniformity of the results might be due to the small range in counts in the fiber-path streak. Note also that the data in Fig. 12 indicate either a slight shot-to shot variation in dispersion, or assigned uncertainties that are too small.

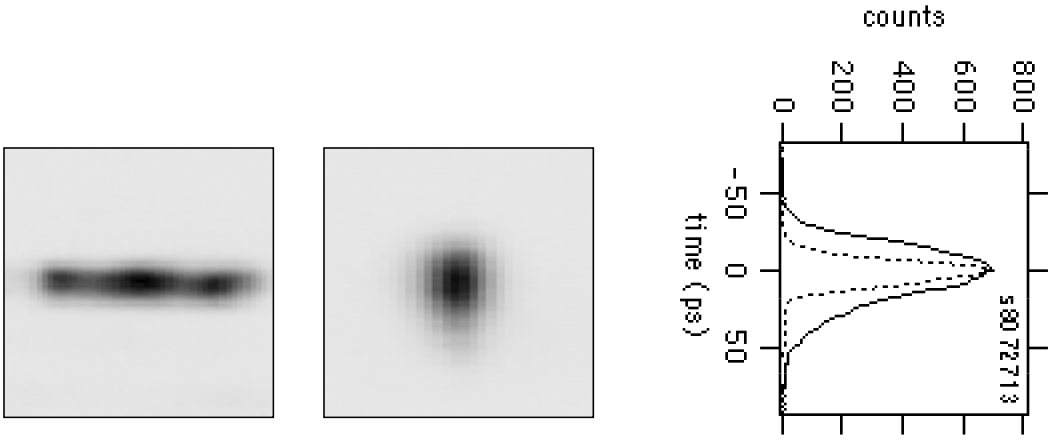

Fig. 10. Left and Center: Excerpts from a streak that was recorded during testing of the 35-m single fiber. Duration (top to bottom) is 160 ps. Right: Pulse waveforms.

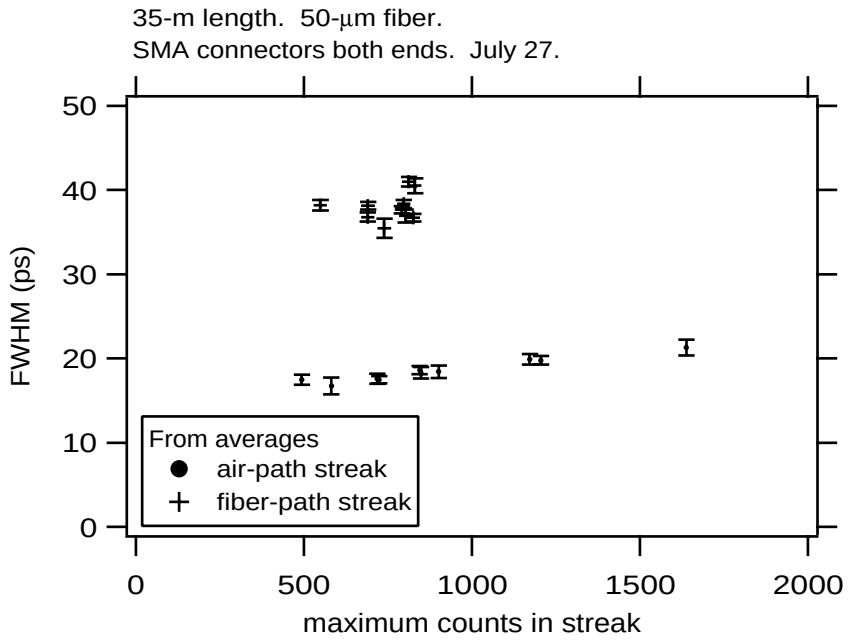

Fig. 11. FWHM vs counts in the streaked images that were recorded during testing of the 35-m single fiber.

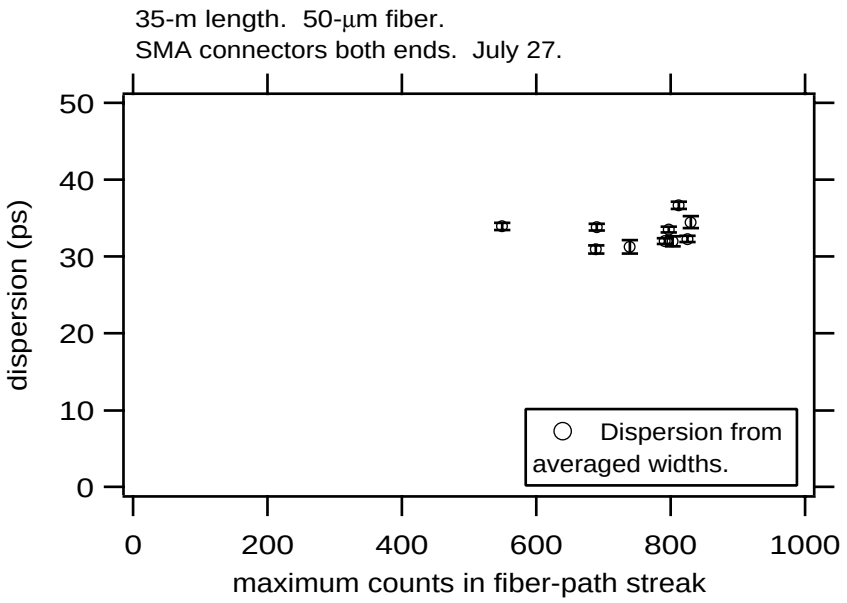

Fig. 12. Measurements of dispersion in a 35-m length of 50-μm-core fiber.

IV.B. Results for the 35-m bundle.

Results for the bundle were quite different. Figures 13 and 14 show streaks of the light that was transmitted by the bundle. The images contain 86 rows corresponding to 160 ps. Figure 13 was recorded at 900 counts. It contains two separate pulses, and the second pulse is laterally displaced. A variety of waveforms can be generated by sectioning this doubled image. All of them have FWHM of about 130 ps, and total duration greater than the 160-ps window.

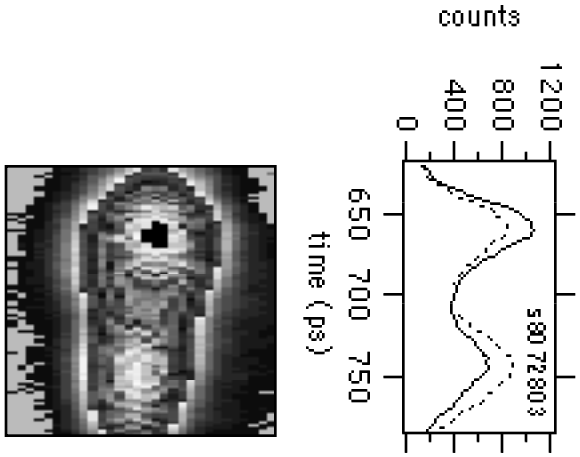

Fig. 13. Left: Segment with duration of 160 ps excerpted from the streak of a pulse that was transmitted by the 35-m bundle. Right: Variation of pulse waveform with column number.

The streak that is shown Fig. 14 was recorded at 400 counts. The second pulse is less distinct, and the FWHM is 50-70 ps.

These two figures provide a general characterization of all of the data from the bundle. Half of the streaks were recorded at about 800 counts, and each of these exhibit two distinct pulses. The remainder were recorded at about 400 counts, and in these the second pulse appears only as an extended tail. A doubled pulse could result from errors in the lengths of some of the 19 fibers in the bundle. The pulse separation, 80 ps, corresponds to a length variation of 16 mm. However, a proposed length variation could not explain why the relative intensity of the two pulses varied with camera exposure, which is presumably proportional to the intensity that was propagated through the bundle.

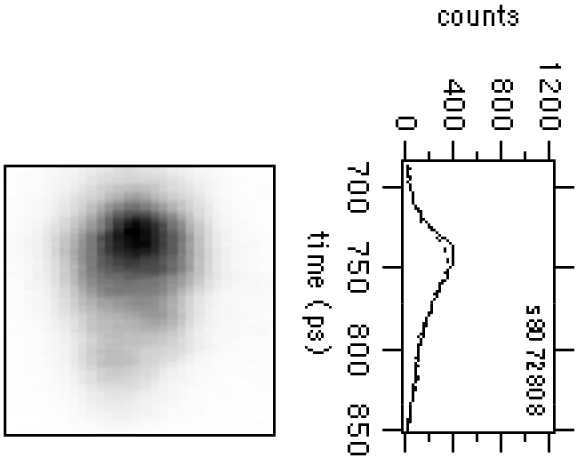

Fig. 14. Left: Segment with duration of 160 ps excerpted from a streak that was recorded at 400 counts during testing of the 35-m bundle. Right: Variation of waveform with column number was slight in streaks recorded at 400 counts or less.

V. Tests of a thick-clad 100-μm-core fiber.

A 50-m length of this fiber was attached to the Launch Optic by an SMA coupler. The other end was cleaved and left unconnectorized. The fiber was tested at four lengths that were obtained by cutting segments from the output end while leaving the SMA input coupler undisturbed. Figure 15 contains the resulting set of 50 values of dispersion. In Fig. 16, these data are represented by mean values and standard deviations. A linear function was fitted to the mean values. If one includes a requirement for zero dispersion at zero length, the dispersion is about 0.8 ps/m.

The individual data from the experiments at the four lengths are contained in Figs. 17-20. All of the streaks were symmetric, and similar uncertainties were observed each of the four experiments.

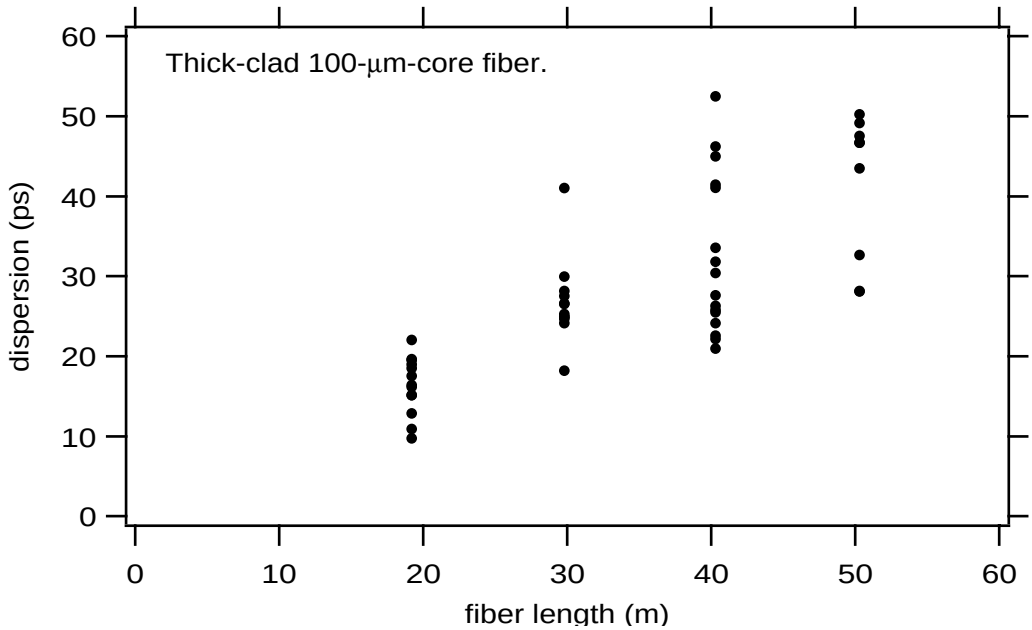

Fig. 15. Summary of 50 measurements of dispersion in a 100-μm-core thick-clad fiber. Details of the measurements for each length are contained in Figs. 17-20.

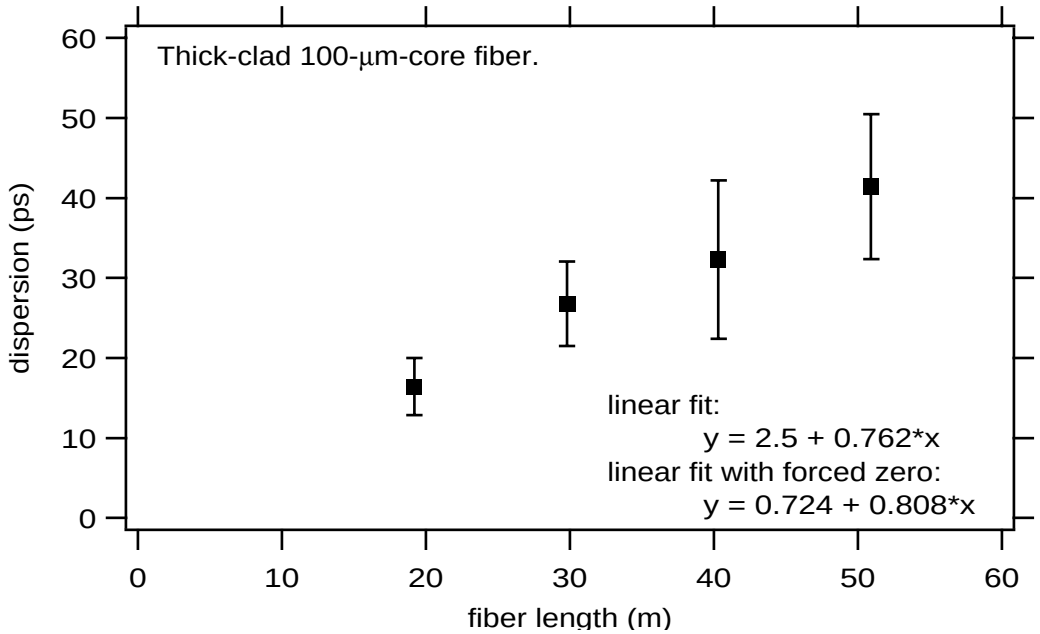

Fig. 16. Median values and standard deviations for the data sets that are shown in Fig. 15. Representation of the data by median values ignores the variation of dispersion with counts, but this treatment is realistic unless we are willing to limit streak exposures to a few hundred counts.

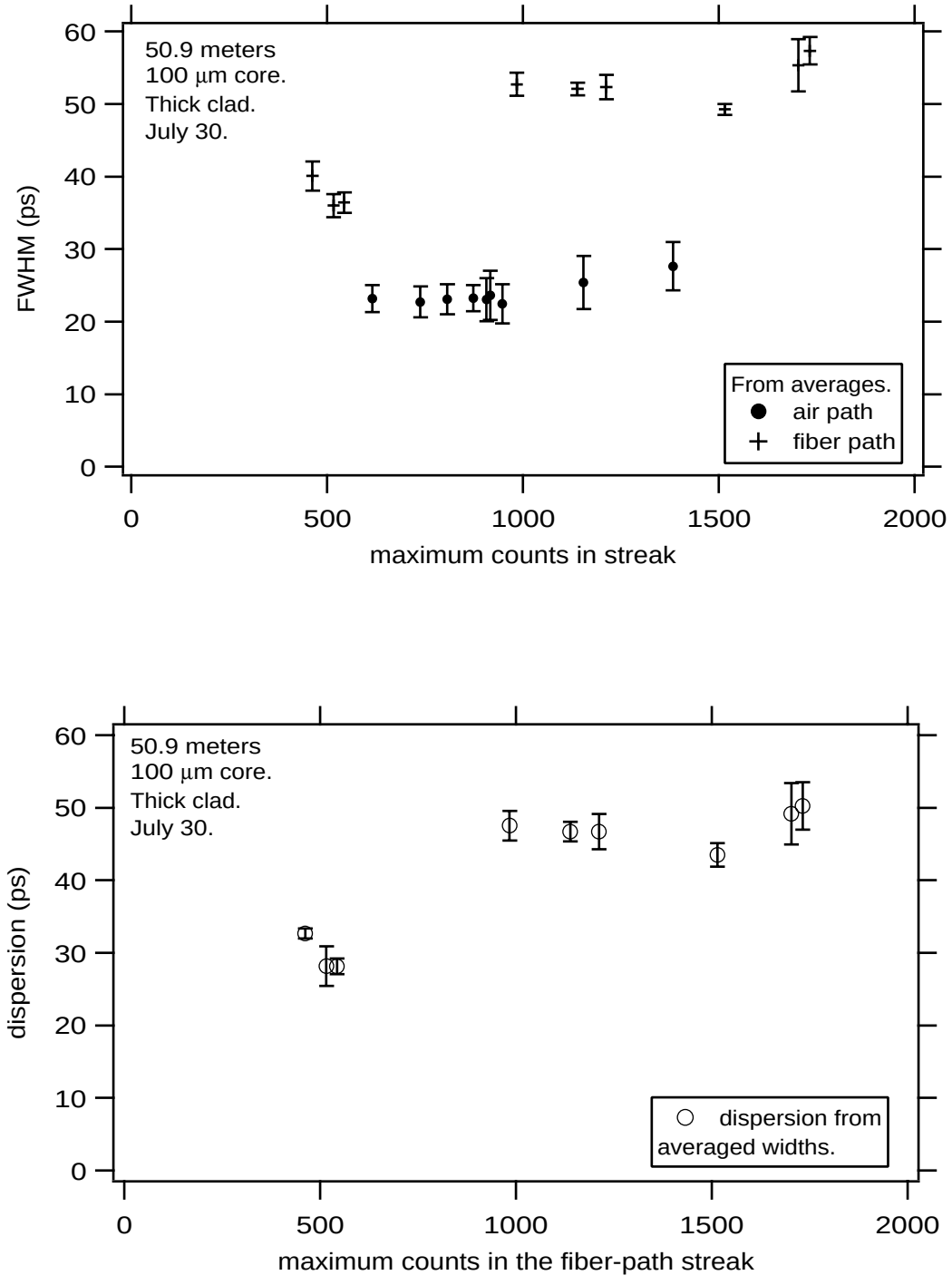

Fig. 17.
Top: FWHM vs counts for streaks recorded during measurements of temporal dispersion in a 50.9-m length of 100-μm-core thick-clad fiber. Each datum is the average of four measurements. The assigned uncertainty indicates the variation in the four measurements. Bottom: Corresponding values of dispersion. Uncertainties indicate the range of values that is allowed by the variation in FWHM.

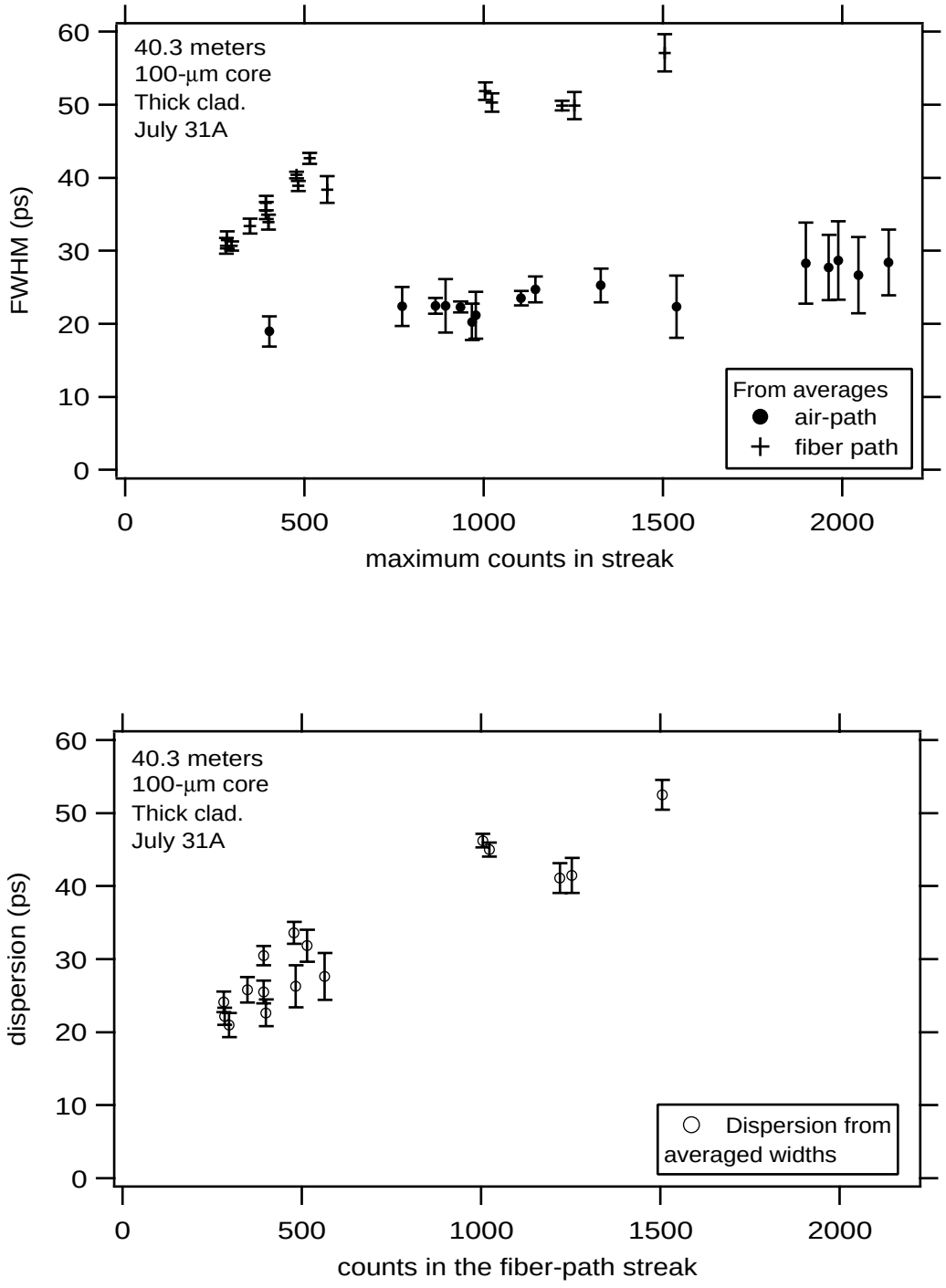

Fig. 18.
Top: FWHM vs counts for streaks recorded during measurements of temporal dispersion in a 40.3-m length of 100-µm-core fiber.
Bottom: Corresponding values of dispersion.

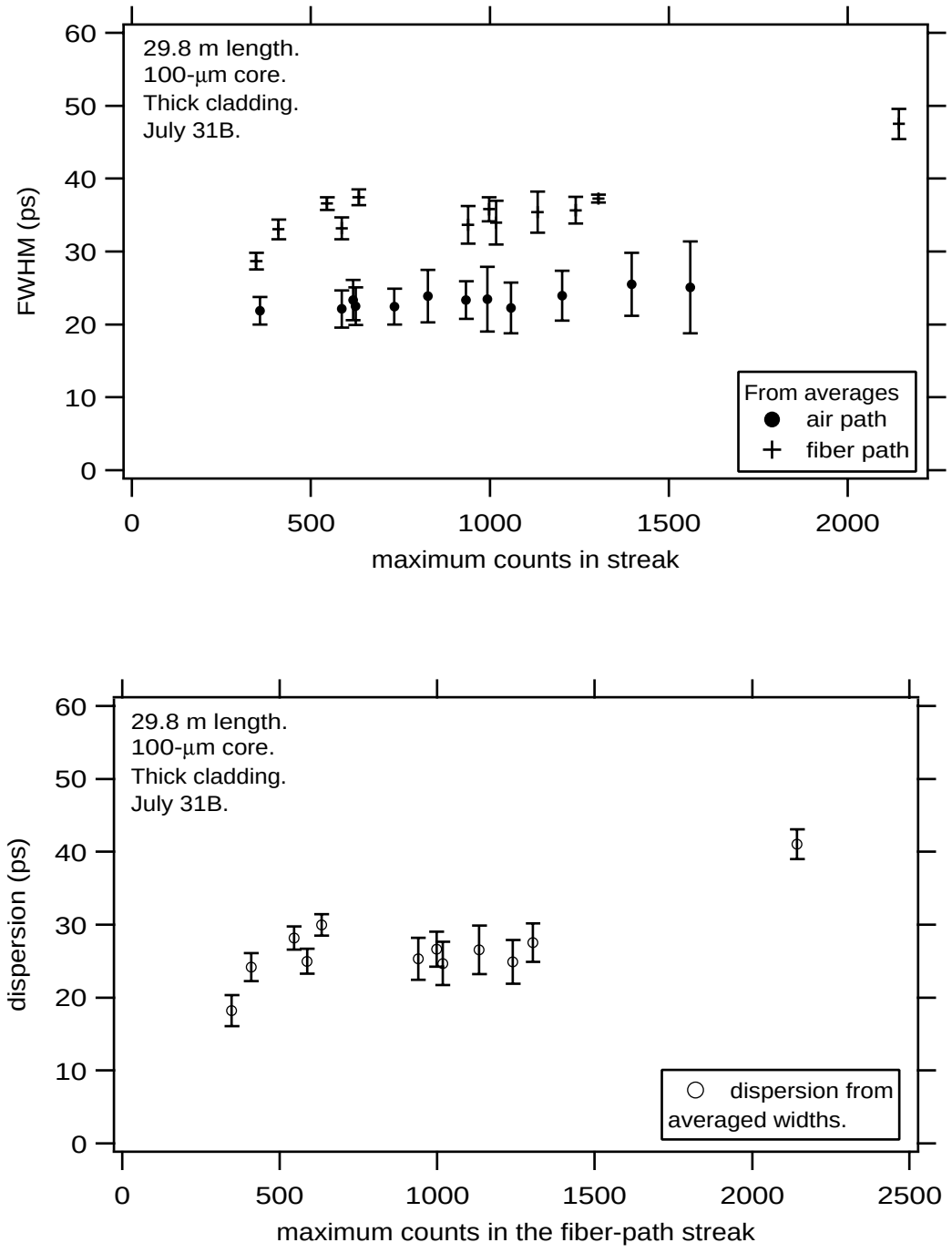

Fig. 19.
Top: FWHM vs counts for streaks recorded during measurements of temporal dispersion in a 29.8-m length of 100-μm-core fiber.
Bottom: Corresponding values of dispersion.

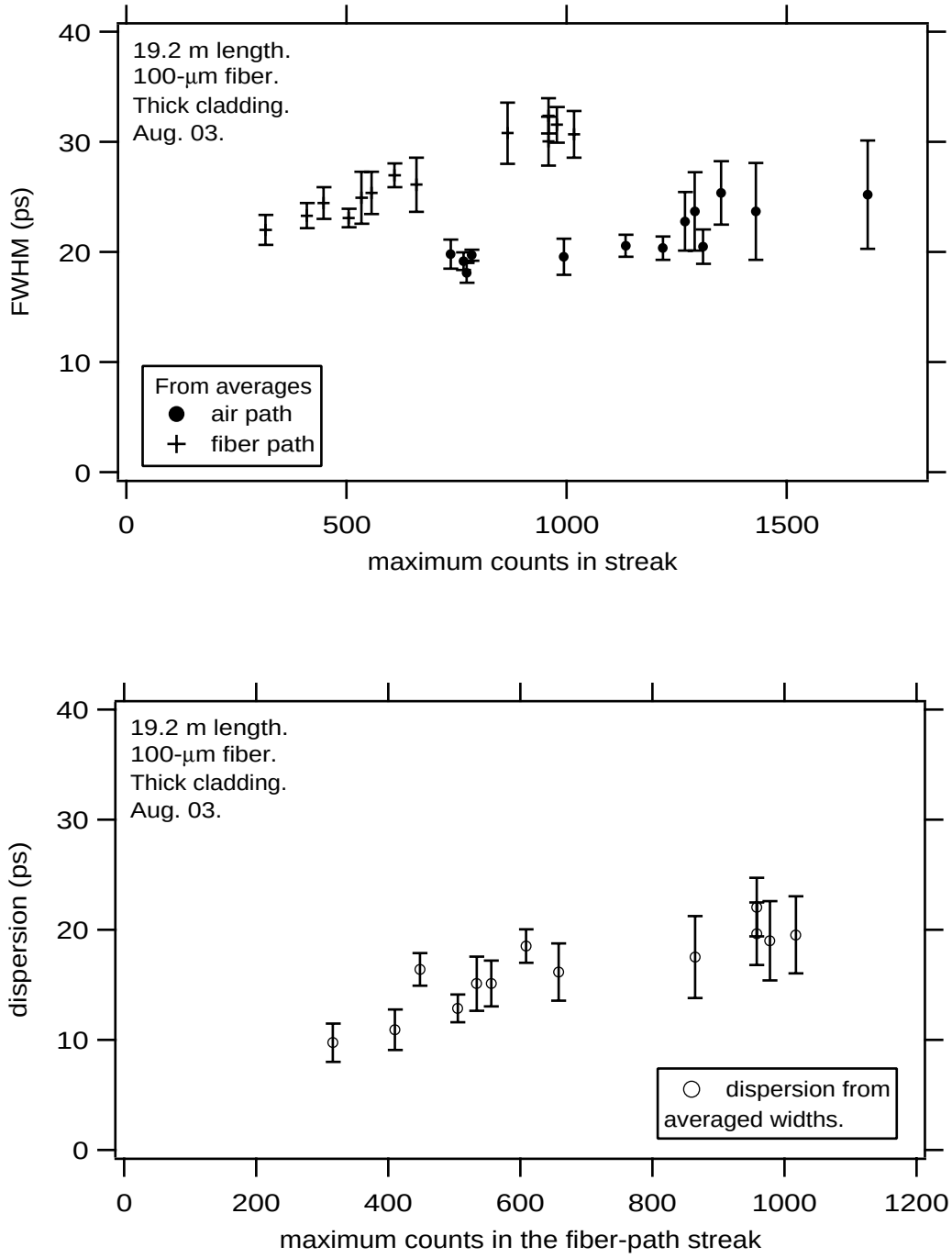

Fig. 20.
Top: FWHM vs counts for streaks recorded during measurements of temporal dispersion in a 19.2-m length of 100-μm-core fiber.
Bottom: Corresponding values of dispersion.

VII. Tests of 50-μm-core fiber samples "B" and "C".

Two samples of the 50-μm-core fiber preform #24 were tested. In the lab notes, these fibers were designated samples B and C. Both were initially about 50 meters in length, and they were delivered to OSL with an SMA connector on one end for attachment to the Launch Optic. The intent was to measure each at 4 lengths, but difficulties were experienced both in cleaving the fibers, and in positioning the cleaved ends in a manner that allowed recording of streaks. We finally managed to test each at 3 lengths.

Fiber C was tested at the 50.4-m length, without difficulty, on Aug. 05. The fiber was cut to a length of 39.8 m, but we were unable to obtain adequate transmittance for streak recordings even with several cleavings of the output end. Believing that we might have damaged the unspooled segment of the fiber, we then cut away an additional 10.54 m, and still were unable to obtain signals. To cover the possibility that the fiber was damaged in the short section between the spool and the Launch Optic, a few meters were cut from that end and the end was terminated. On the last two days of the experiment, this fiber was tested at lengths of 29.3 m and 18.7 m without difficulty.

The collected set of measurements for sample C are in Fig. 21. The data cannot be fitted by a linear function that passes through the origin. The measurements of FWHM and dispersion for the three experiments are shown in Figs. 22-24.

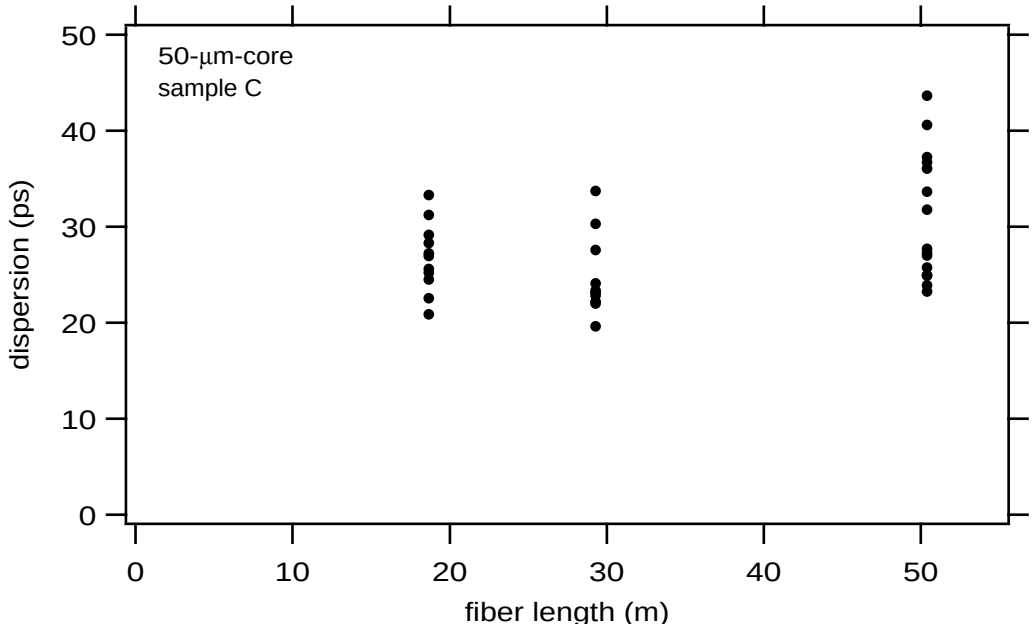

Fig. 21. Collected results of 35 measurements of temporal dispersion in a sample C of the 50-μm-core single fiber.

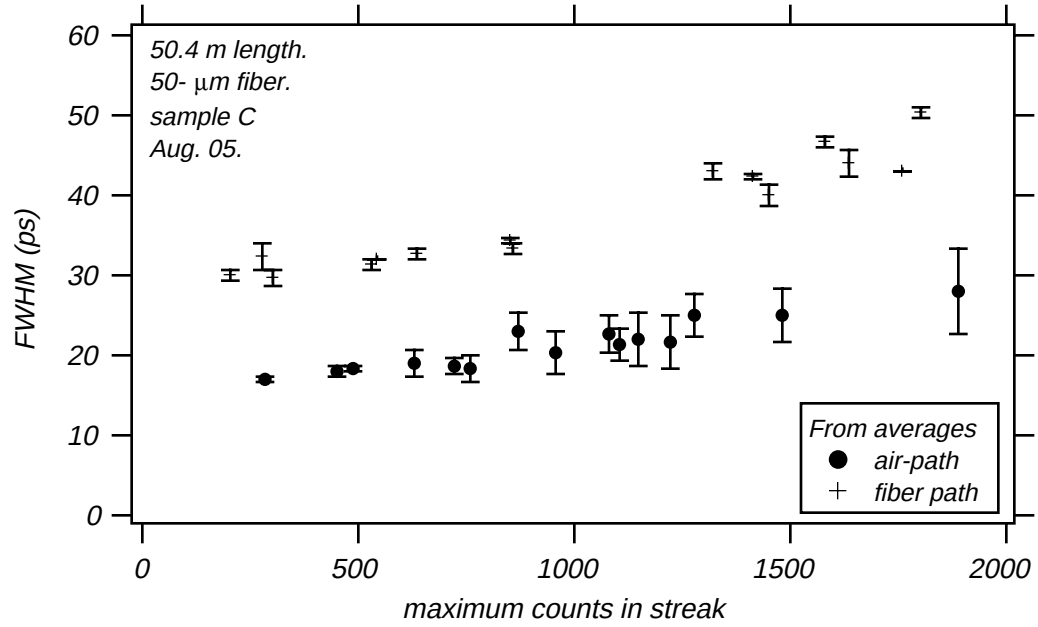

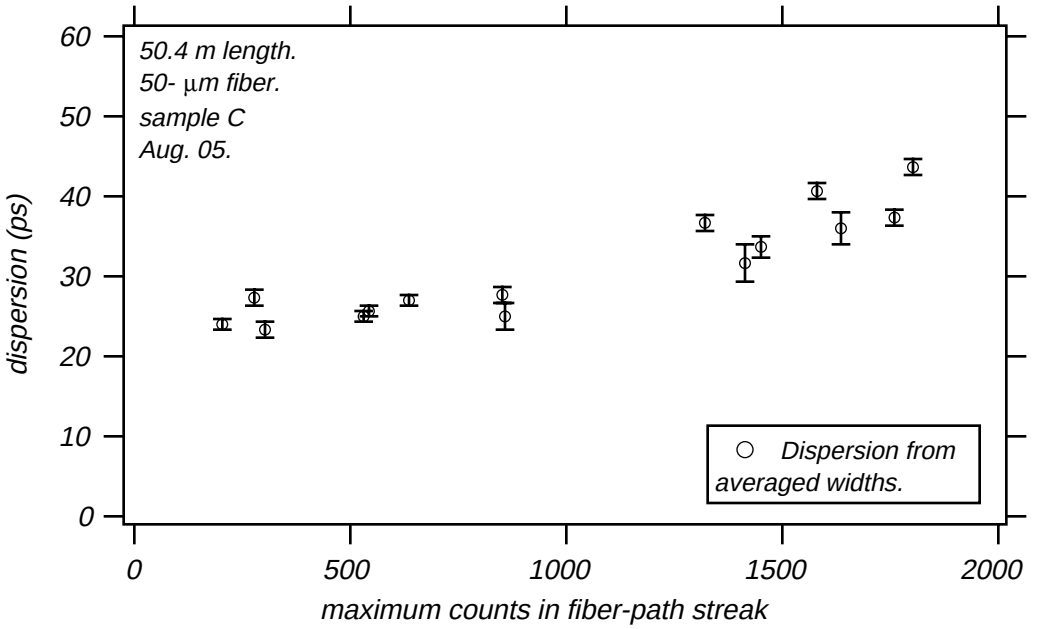

Fig. 22.
Top: FWHM vs counts for streaks recorded during measurements of temporal dispersion in a 50.4-m length of 50-μm-core fiber.
Bottom: Corresponding values of dispersion.

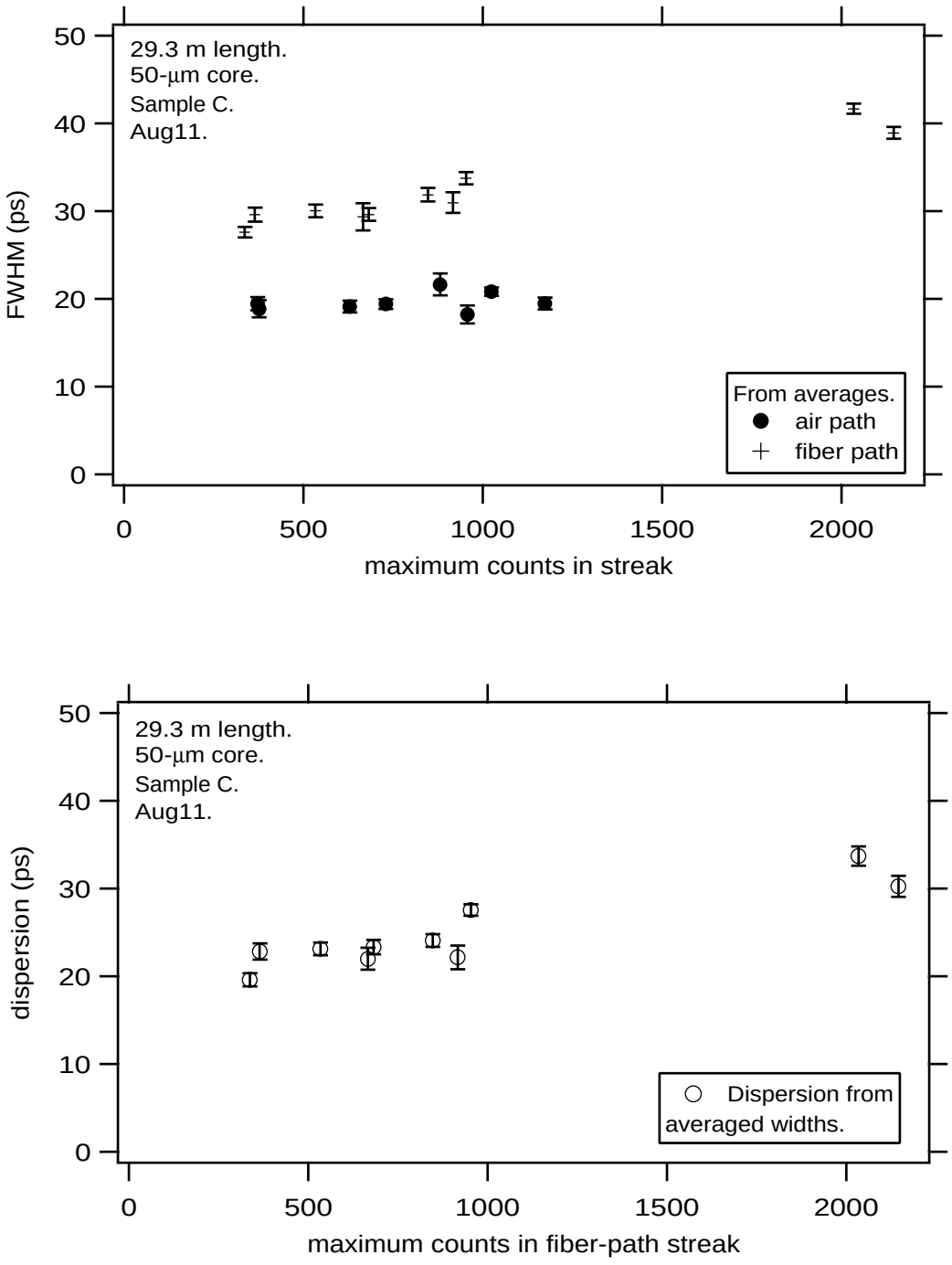

Fig. 23.
Top: FWHM vs counts for streaks recorded during measurements of temporal dispersion in a 29.3-m length of 50-µm-core fiber.
Bottom: Corresponding values of dispersion.

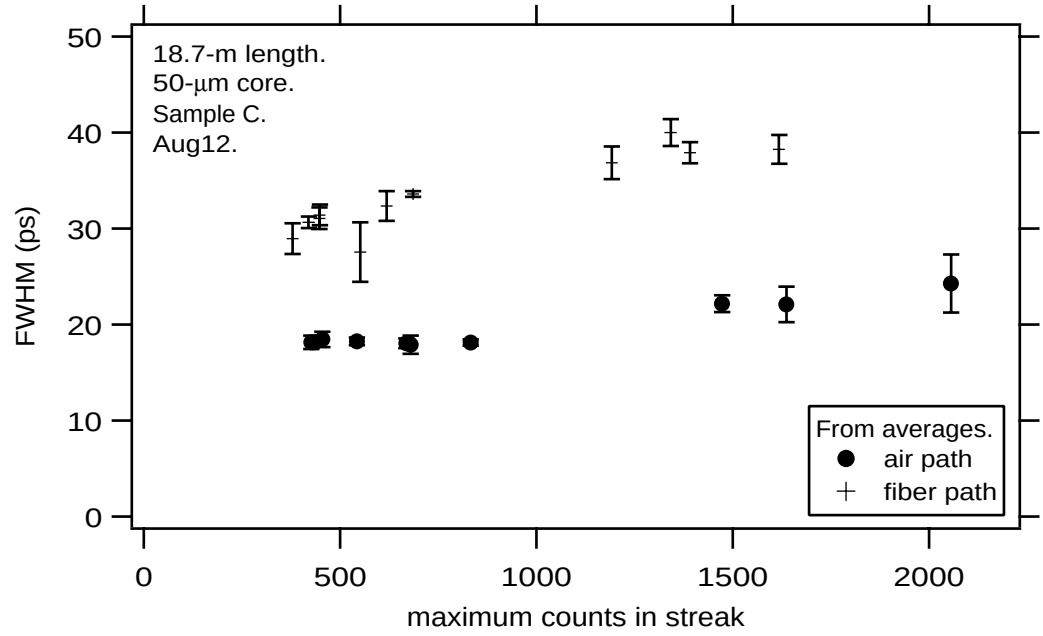

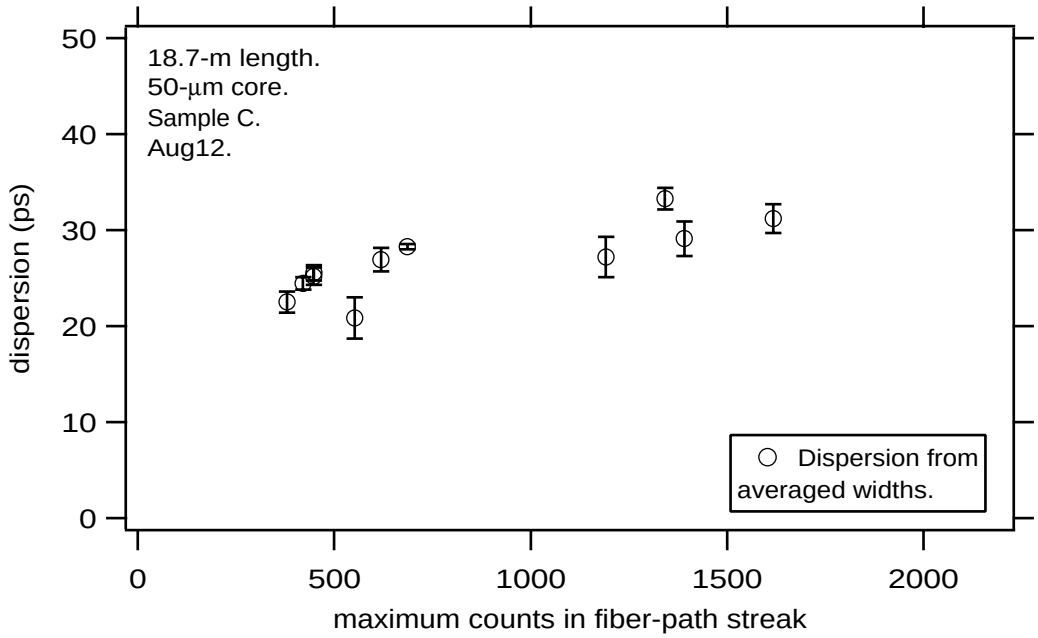

Fig. 24.
Top: FWHM vs counts for streaks recorded during measurements of temporal dispersion in a 18.7-m length of 50-μm-core fiber.
Bottom: Corresponding values of dispersion.

Sample B was tested at the 40.3 meter length on Aug. 06, although many cleavings were required. With a different cleaver (York FK12), data were obtained without difficulty at length of 29.7 m the same day and at 19.1 m the next day. The complete set of data is shown in Fig. 25. They are consistent with dispersion values ranging from 0.8 to 1.2 ps/m.

Results for individual tests are given in Figs. 26-28. They contain a suggestion that the generation of spatially irregular streaks from single fibers is a result of something that we are doing, and not a fundamental characteristic of the fiber. Figures 26 and 28 contain data from the longest and shortest segment of this fiber. The fiber-path streaks were spatially uniform, and the uncertainty in the measurement of FWHM was small. Figure 27 contains data for the experiment with the intermediate length. The streaks were spatially irregular and the uncertainties in FWHM were large.

These experiments were not interrupted, and we attempted to leave the SMA coupling to the Launch Optic undisturbed. Therefore, the primary differences are that each test was made with unique end cleaves and with unique positionings of the fiber end at the slit of the streak camera. It seems that we should be able to avoid the problem of irregular streaks in future tests. However, even the noisy data in Fig. 27 indicate that the dispersion increased with counts, so that observation is not likely to be changed by the obtaining of uniform streaks.

VIII. Reference.

1. D. Milam, Walter Sell, Alan Gates, and Leslie Summers, "Fiber-Optic System for Measuring Power Balance: Evaluation of the Launch Optics, Fiber Bundles, and the Multiple-Port Fiber-to-Diode Multiplexer," NIF - 0014454, WBS 1.7.2.2.4, Sept. 22, 1998.

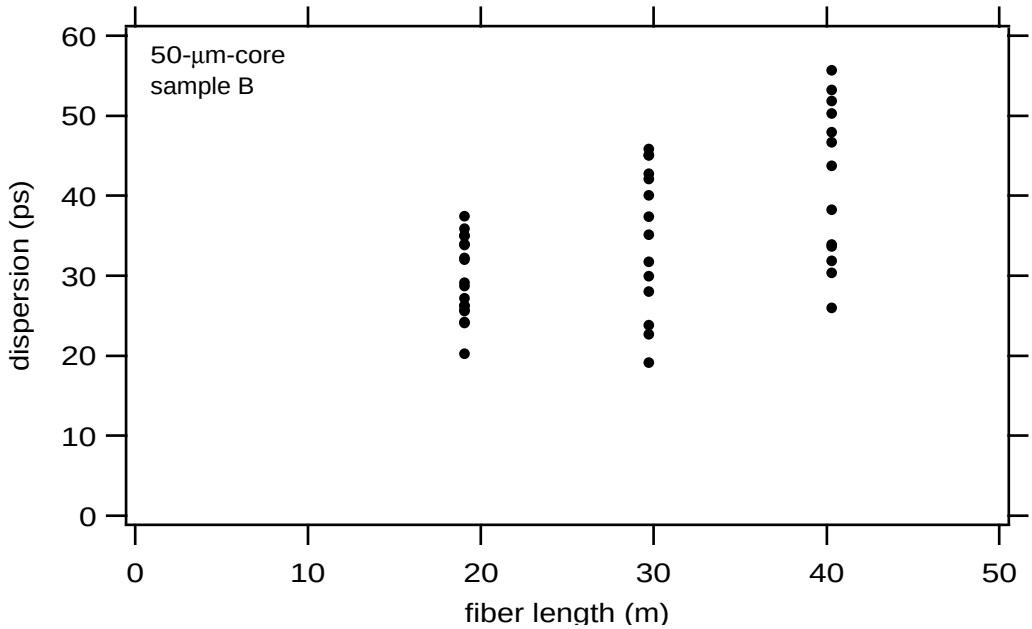

Fig. 25. Collected results of 44 measurements of temporal dispersion in sample B of the 50-μm-core fiber.

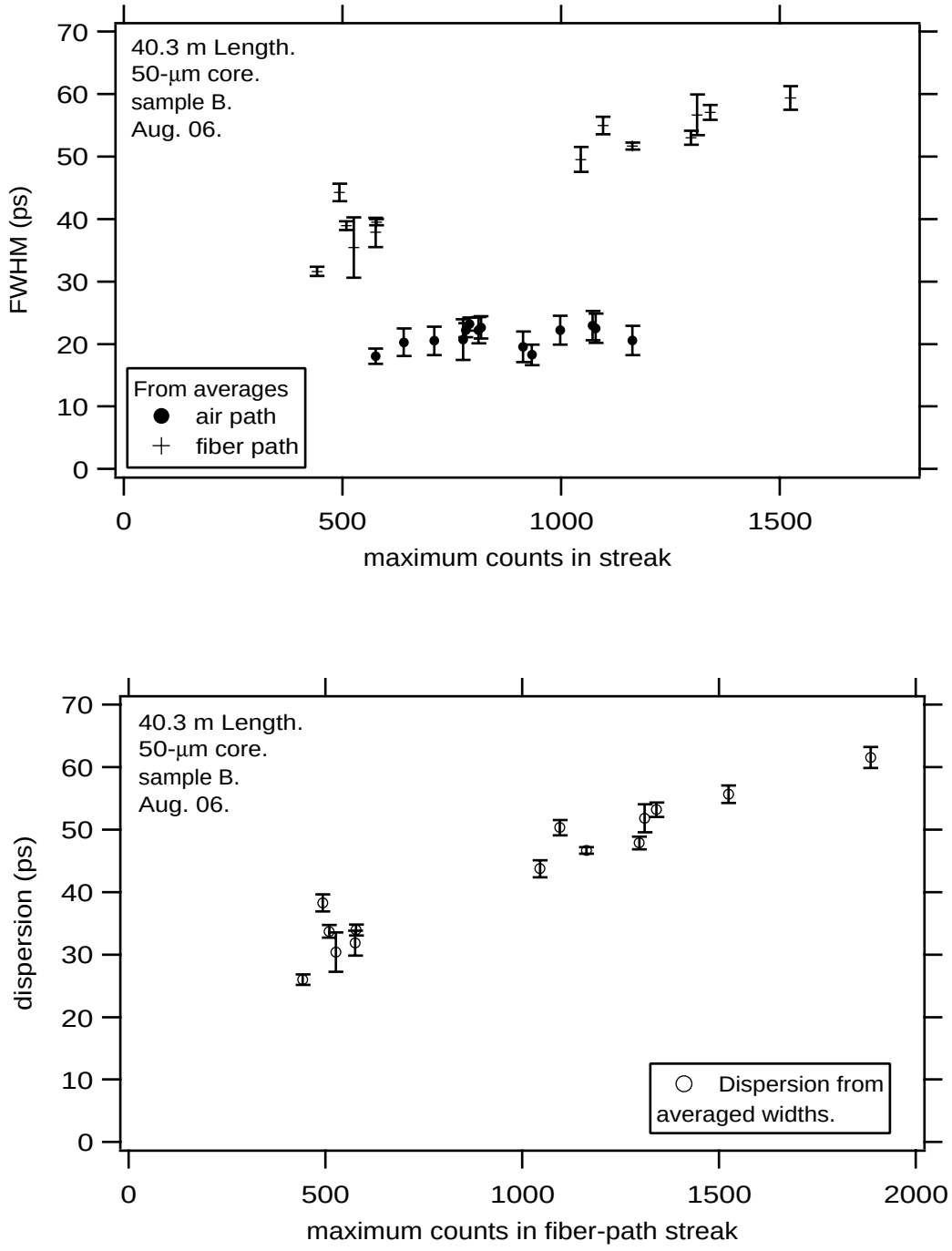

Fig. 26.
Top: FWHM vs counts for streaks recorded during measurements of temporal dispersion in a 40.3-m length of 50-μm-core fiber (sample B).
Bottom: Corresponding values of dispersion.

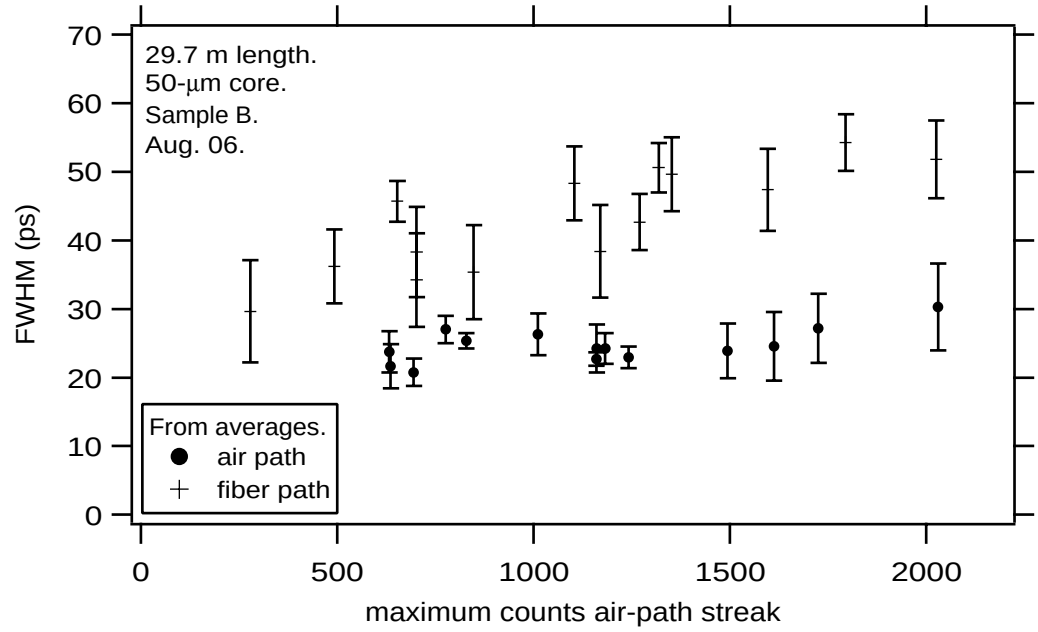

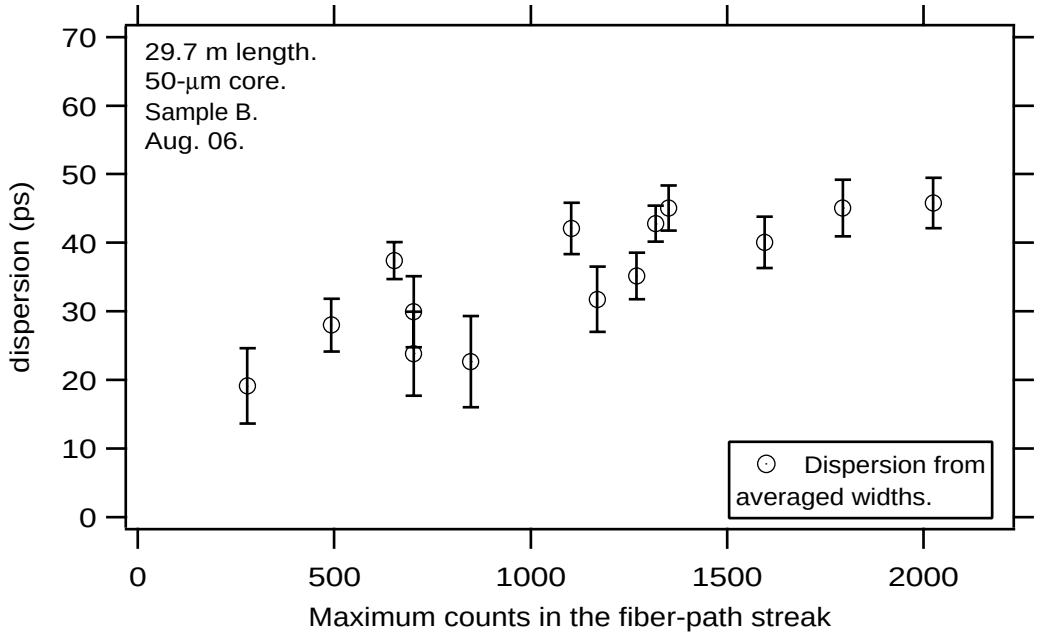

Fig. 27.
Top: FWHM vs counts for streaks recorded during measurements of temporal dispersion in a 29.7-m length of 50-μm-core fiber (sample B).
Bottom: Corresponding values of dispersion.

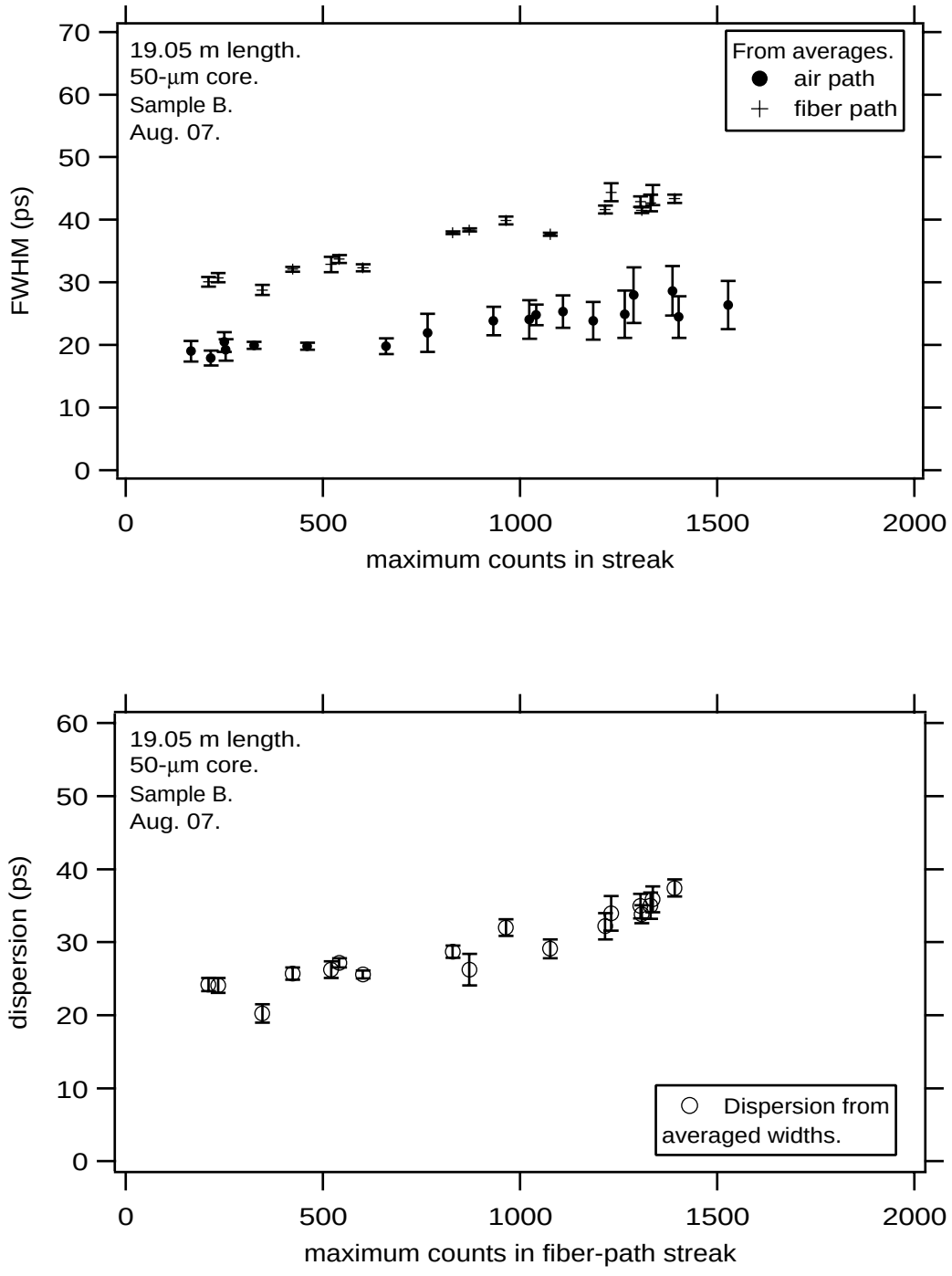

Fig. 28.
Top: FWHM vs counts for streaks recorded during measurements of temporal dispersion in a 19.1-m length of 50-µm-core fiber (sample B).
Bottom: Corresponding values of dispersion.